Liquid Crystals
Publication details, including instructions for authors and subscription information:
http://www.informaworld.com/smpp/title~content=t713926090

Gradient flexoelectric switching response in a nematic phenyl benzoate

Pramoda Kumar[a]; K. S. Krishnamurthy[a]
[a] Centre for Liquid Crystal Research, Jalahalli, Bangalore 560 013, India

To cite this Article Kumar, Pramoda and Krishnamurthy, K. S.(2007) 'Gradient flexoelectric switching response in a nematic phenyl benzoate', Liquid Crystals, 34: 2, 257 — 266
To link to this Article: DOI: 10.1080/02678290601111192
URL: http://dx.doi.org/10.1080/02678290601111192

Liquid Crystals, Vol. 34, No. 2, February 2007, 257–266

Gradient flexoelectric switching response in a nematic phenyl benzoate

PRAMODA KUMAR and K. S. KRISHNAMURTHY*
Centre for Liquid Crystal Research, PO Box 1329, Jalahalli, Bangalore 560 013, India

(*Received 15 August 2006; accepted 8 October 2006*)

We report on the inverse flexoelectric effects observed in a nematic liquid crystal with a small positive dielectric anisotropy subject to static and very low frequency (<1 Hz) a.c. fields. The Bobylev–Pikin flexobands appear at a temperature-dependent d.c. threshold. Under square wave excitation, a new type of transient optical response occurs soon after each polarity reversal, and we ascribe it to the gradient flexoelectric distortion explicable on the basis of the presence of intrinsic double layers. This instability is characterized by a threshold voltage that decreases with temperature. Its maximum amplitude increases linearly with voltage close to threshold, and occurs after polarity reversal at a time τ_m that scales inversely as the voltage; τ_m decreases exponentially with frequency and temperature. After each polarity change, the ionic current following the charging current decreases almost exponentially to a non-zero value; the residual current increases monotonically with the applied bias.

1. Introduction

A strain-free nematic is invariant with respect to the director inversion, $\mathbf{n}\rightarrow-\mathbf{n}$. Curvature deformations of the splay and bend type could break this symmetry and lead to a non-vanishing local polarization of the medium. Flexoelectric polarization may arise from a coupling between molecular shape asymmetry and permanent dipolar moments [1]; it may also be due to an asymmetry in the assembly of the electric quadrupoles in the presence of curvature strains [2]. Under certain conditions, an inverse flexoeffect is produced in which an applied electric field generates a curvature strain of the splay, bend or splay–bend type in a nematic. Flexoelectric torque due to an applied field $\mathbf{E}$ is conveniently expressed as $\mathbf{n}\times\mathbf{h}$ with $\mathbf{h}$, the molecular field, given by

$$\mathbf{h}=(e_s-e_b)(\mathbf{E}\nabla\,.\,\mathbf{n}-\nabla\mathbf{n}\,.\,\mathbf{E})-(e_s+e_b)\mathbf{n}\,.\,\nabla\mathbf{E}. \quad (1)$$

Here e_s and e_b are the flexoelectric coefficients appropriate to the splay and bend distortions, respectively [3]. While the first term on the right hand side of this expression is relevant for the flexoeffect induced by a homogeneous electric field, the second term is responsible for the so-called gradient flexoelectric effect (GFE) produced by an inhomogeneous field [3–7].

We have conducted electro-optical experiments, under both uniform and varying field conditions, on the flexoinstabilities in a planar nematic with a small dielectric anisotropy, ε_a. Our primary purpose here is to present and discuss a novel transient switching response attributable to the GFE. For comparison, we also report results pertaining to the homogeneous field experiments.

Transient director switching in nematic liquids has been the subject of numerous experimental and theoretical investigations. However, in most of these studies the alignment distortion arises from the dielectric torque, which is quadratic in the field; moreover, attention is predominantly focused on transient current effects [8, 9], rather than associated electrooptic responses [10], that follow polarity reversals. The first significant report of gradient flexoelectric (GF) optical modulation in a nematic was by Derzhanski *et al.* [5]. However, this modulation was due to the steady state field inhomogeneity, and persisted as long as the static field existed. As far as we know, the only report to date of a transient optical effect occurring at polarity reversals and attributable to the GFE is by Basappa and Madhusudana [11], who investigated a nematic with a strong positive ε_a in the dielectrically stable configuration. The switching phenomenon observed here differs significantly from the one studied by them as will be discussed at the end of § 3.

2. Experimental

We used a reagent grade sample of butyl *p*-(*p*-ethoxyphenoxycarbonyl)phenyl carbonate (BEPC)

*Corresponding author. Email: murthyksk@gmail.com

Liquid Crystals
ISSN 0267-8292 print/ISSN 1366-5855 online © 2007 Taylor & Francis
http://www.tandf.co.uk/journals
DOI: 10.1080/02678290601111192

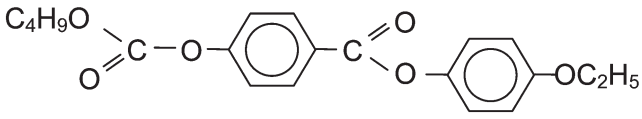

supplied by Eastman Organic Chemicals. It exhibited an enantiotropic nematic phase between *c.* 55 and 84°C. The sample cells were sandwich type, constructed of ITO coated glass plates. Unless otherwise specified, the substrate glass may be taken as passivated with SiO_2 layers before application of the ITO coatings (from Delta Technologies), and used with no blocking layers. Mylar spacers, heat-sealed to the electrodes through cooling from *c.* 250°C under a uniform pressure, determined the cell spacing, d. The d-value was determined interferometrically, using a channelled spectrum. For securing a planar alignment, the electrodes were rubbed unidirectionally before cell construction. The easy axis is taken as the reference direction x. Observations were carried out in transmitted mercury light, along z, the layer normal, using a Leitz DMRXP polarizing microscope, equipped with a Sony CCD camera and a Mettler FP90 hot-stage. The electric field was applied along $\pm z$. The voltage source was a Stanford Research Systems DS 345 function generator coupled to a FLC Electronics voltage amplifier (Model F20ADI). The applied voltage was measured with a HP 34401A multimeter.

The dielectric anisotropy of BEPC has been reported to vary from about 0.21 at the melting temperature to 0.06 at 84°C [12]. The results of our independent dielectric measurements on BEPC agreed with the reported data to within 5%. The resistivity of BEPC at 75°C was $\sim 5 \times 10^9\,\Omega\,\mathrm{cm}$. The birefringence of BEPC has been reported as ranging between 0.141 at 56°C and 0.087 at 83°C [13].

For convenience, when the polarizer has its transmission axis along x and the analyser along y, it will be represented as P(x)-A(y); P(45)-A(135) indicates the diagonal setting of P and A, with the angles in parentheses in degrees measured from the x-direction.

3. Results and discussion

3.1. *Flexoelectric bands due to a static field*

In a steady electric field, above a well defined voltage threshold V_f, thin samples display parallel bands along the initial alignment direction x with periodicity along y, as in figure 1. This instability, arising in planarly aligned and strongly anchored samples, was first explained by Bobylev and Pikin [4, 14] as a volume effect, involving a two-dimensional deformation characterized by the director deviation away from x, by an

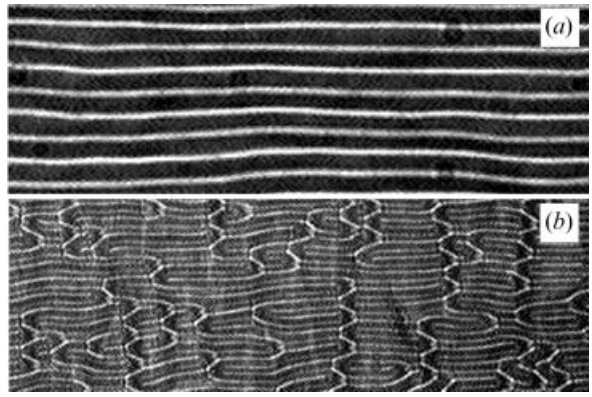

Figure 1. Focal lines due to volume flexoelectric domains in BEPC under a static field at 55°C. Parallel polarizers set along x, d=7.5 μm. (*a*) 7.53 V, (*b*) 20.1 V.

angle φ in the xy-plane and θ in the xz-plane. The director field is defined by $\theta=\theta_o \cos(qy)\cos(\pi z/d)$ and $\varphi=\varphi_o \sin(qy)\cos(\pi z/d)$, where q is related to the spatial frequency or domain density κ by $q=\pi\,\kappa$. In figure 2 we present the dependence of κ on V; the linear scaling seen here is in consonance with the theoretical prediction in [14]. In fact, a similar behaviour has long since been known in several nematics [15–18], including a quaternary mixture of phenyl benzoates with BEPC as a component [18]. However, BEPC differs from several other nematics with regard to the temperature variation of the Bobylev–Pikin (BP) threshold, V_f.

We may recall here that, under elastic isotropy condition, V_f is given by [4]

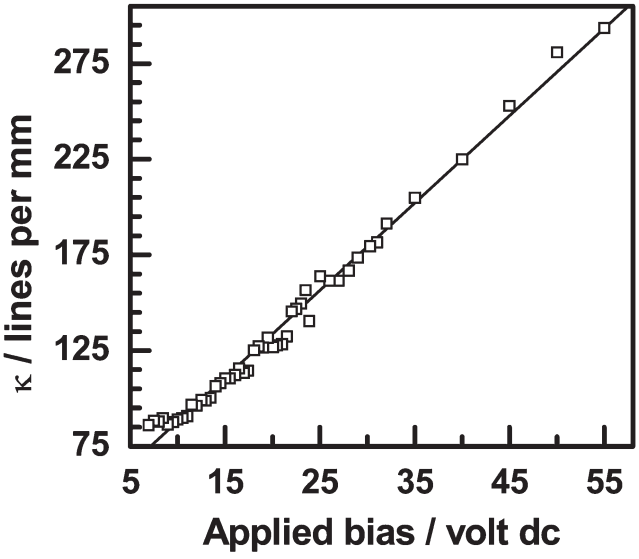

Figure 2. Domain focal-line density as a function of applied voltage for a 7.5 μm thick sample at 55°C.

$$V_f = \frac{2\pi k}{e(1+v)}, \quad v = \frac{\varepsilon_0 \varepsilon_a k}{e^2} \tag{2}$$

with k as the elastic modulus under one-constant approximation and e denoting $|e_s - e_b|$. Hence, when ε_a is small and $v << 1$, V_f is expected to vary with temperature in the same manner as k/e. For an azoxy compound, Barnik *et al.* [18] have found V_f to be almost temperature independent; they explain this as due to identical temperature variations of k and e. However, for BEPC, we find a definite increase in V_f with temperature, almost up to the clearing temperature as in figure 3. It is known that k is quadratic in the order parameter $S(T)$; further, from the molecular theory of dipolar flexoelectricity [7], e_s and e_b are expressible, respectively, as $[aS^2(1+2S)/T]$ and $[bS^2(1+S/2)/T]$, where a and b are constants involving components of dipole moment and shape anisotropy of molecules appropriate to splay and bend deformations. Therefore,

$$\frac{k}{|e|} \propto \frac{T}{|(a-b)+(2a-b/2)S|} \tag{3}$$

and the behaviour in figure 3 is not surprising. Additionally, if the anisotropy of elastic coefficients is also considered, for compounds with $\varepsilon_a > 0$, theoretically [4], V_f should show a nonlinear increase with k_2/k_1, the ratio of twist to splay modulus (or temperature, by implication). But how do we understand the slight decrease in V_f close to the nematic–isotropic point? In fact, a number of nematogens have been observed experimentally to show a negative temperature coefficient of k/e, with e varying more like S than S^2; this behaviour has been attributed to a relative increase in the number of conformations producing bent structures with elevation in temperature [19].

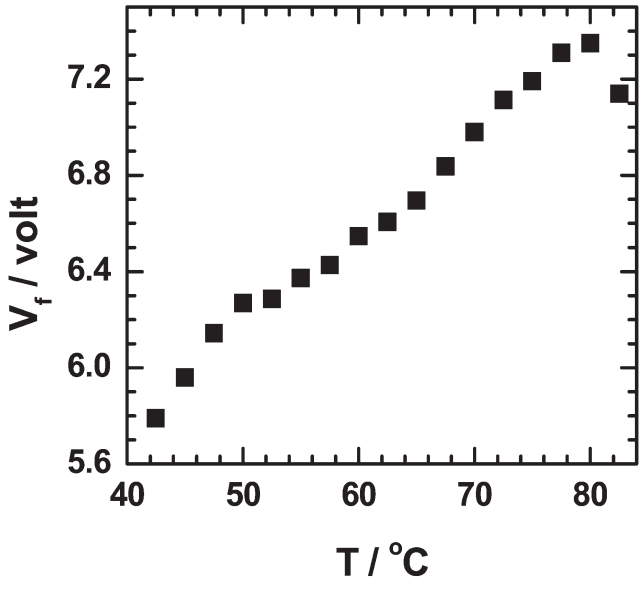

Figure 3. Temperature dependence of volume flexoelectric threshold. The sample is in the supercooled nematic state below 55°C.

The threshold period of volume flexobands, Λ, may be expressed in terms of V_f as [4]

$$\pi\left(1 + \frac{d^2}{\Lambda^2}\right) = \frac{eV_f}{k}. \tag{4}$$

Keeping the temperature constant at 55°C, we studied V_f as a function of d/Λ and obtained the value of $0.62\,\mathrm{C\,N^{-1}\,m^{-1}}$ for e/k; from the Fréedericksz threshold and ε_a values at the same temperature, we determined k to be $\sim 9.6 \times 10^{-12}\,\mathrm{N}$, so that e is $\sim 5.95 \times 10^{-12}\,\mathrm{C\,m^{-1}}$.

3.2. *Gradient Flexoelectric switching in low frequency fields*

In samples subject to a constant field of low voltage amplitude ($< V_f$), no alignment distortion is observed. However, immediately after the field is turned on and before the steady state is reached, the nematic director undergoes a transient angular excursion. This is inferred from the momentary down-shift of the birefringence colour of the sample held between diagonally crossed polarizers. It appears therefore that, at low voltages, during the counterion transport, the electric field inhomogeneity is extensive enough to cause an observable change in the phase difference; as the steady condition is approached, the field tends to become uniform in bulk; and the gradients that eventually exist close to the electrodes are confined to regions so narrow that no perceptible flexoresponse is elicited. These observations are better appreciated in figure 4 illustrating a typical electro-optic response in a sample subjected to a 5 mHz square wave field. Clearly, the switching occurs at double the frequency of the driving field and, except for a relatively short switching period following each polarity reversal, the planar alignment remains practically undisturbed during the constancy of voltage. Further, the distortion amplitude, while remaining the same for alternate switching events, differs for successive events. For instance, in figure 4, the half-intensity width is different for the two switching peaks, being ~1.6 s for the left peak and 2.4 s for the right one. This asymmetrical response is possibly a reflection of the slightly dissimilar conditions prevailing at the two substrates.

The birefringence colour of the sample to which figure 4 refers is second order green in the field off state, as shown in figure 5 (*a*). The snapshots in figures 5 (*b*)–5 (*d*) were taken during the continual change of birefringence colour occurring in the switching process.

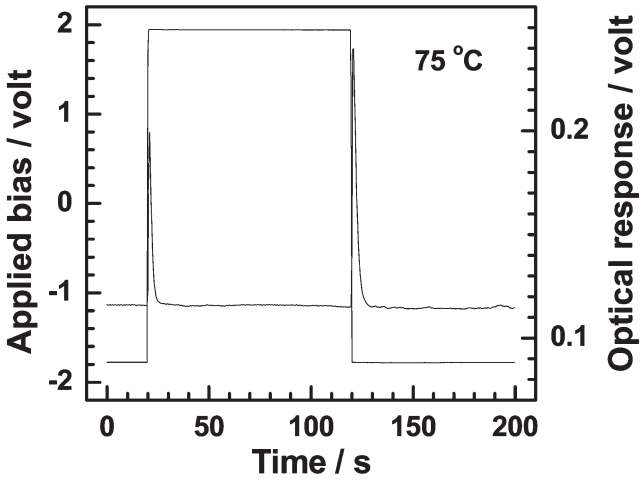

Figure 4. Transient switching response in a 7.75 μm thick layer of BEPC held at 75°C between diagonally parallel polarizers, P(45)-A(45), and driven by a 0.005 Hz square wave field. The relative intensity of transmitted light (right hand scale) reveals a momentary birefringence change following each polarity reversal.

The homogeneous nature of distortion at lower voltages, indicated by the uniformity of colour change in figures 5 (*b*) and 5 (*c*), is analogous to that characterizing the usual Fréedericksz transition. At higher voltages, the transient distortion involves a patterned state and its initial appearance is discernable in figure 5 (*d*).

Figure 6 shows the optical response for various voltage amplitudes of the applied square wave field of frequency 0.05 Hz. Before discussing it, it is useful to recall that, for a nematic single crystal with $\mathbf{n}=(\cos\theta, 0, \sin\theta)$, situated between crossed polarizers, the transmittance T_r is given by

$$T_r = \sin^2 2\alpha \sin^2\left[\frac{\pi d}{\lambda}\left(\frac{n_o n_e}{(n_e^2\sin^2\theta + n_o^2\cos^2\theta)^{\frac{1}{2}}} - n_o\right)\right] \quad (5)$$

where α is the angle made by the incident electric vector with the x-axis. When the alignment is distorted with $\theta=\theta(z)$ and $\alpha=45^\circ$,

$$T_r = \sin^2\frac{\pi L}{\lambda} = \sin^2\frac{\delta}{2};$$
$$L = \int_0^d \left(\frac{n_o n_e}{[n_e^2\sin^2\theta(z) + n_o^2\cos^2\theta(z)]^{\frac{1}{2}}} - n_o\right) dz. \quad (6)$$

Here L is the effective path difference due to the sample in which a splay-Fréedericksz-like distortion is present and δ is the corresponding phase difference. In the rest state, $\theta=0$ and the phase difference $\delta=(2\pi/\lambda)(n_e-n_o)\,d$; assuming (n_e-n_o) at 65°C to be 0.128 [13], the off-state δ for $\lambda=0.546\,\mu$m and $d=7.75\,\mu$m (as in figure 6) is thus 3.6 π, and $T_r=0.345$.

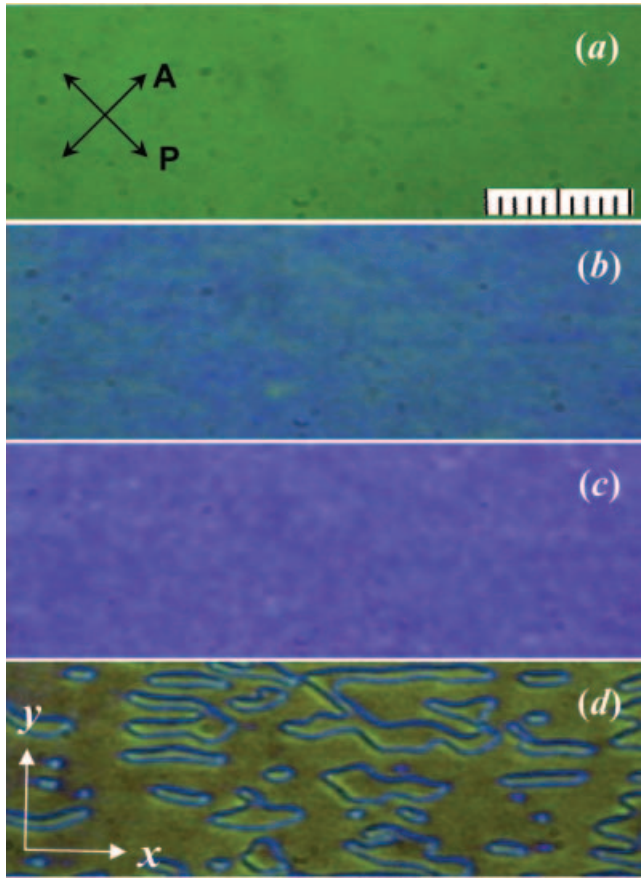

Figure 5. Birefringence colours for incident mercury light (unfiltered) in a 7.75 μm thick sample held between ITO-coated plates with passivation layers. Applied bias: (*a*) 0 V, (*b*) 2.04 V, (*c*) 3.07 V, (*d*) 4.11 V. 10 μm/scale division, 75°C.

We now turn to the optical response profiles in figure 6. During the switching excursion of the director, its tilt-amplitude determines δ_m, the minimum phase difference reached; δ_m is greater than 3π in figures 6 (*a*) and 6 (*b*) since the peak intensity, compared with figure 6 (*c*), is below the maximum possible. In figure 6 (*c*), the two birefringence maxima evidently occur during the rise and fall of the director deviation, at the δ-position of 3π; further, considering that the initial transmittance at $\delta=3.6\ \pi$ recurs next at $\delta=2.4\ \pi$ and that the transmittance at the minimum A in figure 6 (*c*) is greater than its initial value, we may conclude that the corresponding δ_m lies between 2.4π and 3π. The profile in figure 6 (*d*) is similar to that in 6 (*c*), except that the birefringence minimum is now below the base line; this situation corresponds to $2\pi<\delta_m<2.4\pi$. For applied bias above ~6 V, the transient switching is found to occur within the BP patterned state. The latter causes a shift in

the d.c. level. For instance, in figure 6 (*e*), the d.c. level of the optical signal has increased considerably, while in figure 6 (*f*) it is lowered. A close examination of these levels would indicate the initial δ to lie between 2.4π and 3π in figure 6 (*e*), and 2π and 2.4π in 6 (*c*). The δ_m value is likely to be between π and 2π for the switching profiles in figures 6 (*e*) and 6 (*f*).

We may now discuss the homogeneous and periodic GF instabilities in some detail to appreciate better the above observations. Derzhanski and Petrov [6] have shown that a planar nematic liquid crystal can, under certain conditions, display a gradient flexoelectric *volume* instability that mimics the splay-Fréedericksz distortion. For example, when ε_a is 0, the competition is only between the elastic and GF torques; and when the electric field increases linearly from E_c at the cathode to E_a at the anode, the balance of torques yields the threshold V_G of GFE [6]:

$$V_G = \frac{\pi^2}{2}\left(\frac{E_a + E_c}{E_a - E_c}\right)\frac{k}{e^*}; \quad e^* = e_s + e_b. \tag{7}$$

The value of k/e^* mentioned for different nematic materials in [3] ranges roughly between 0.2 and $1\,\mathrm{N\,m\,C^{-1}}$. Therefore, if we take E_a/E_c to be 10 for argument, V_G will be of the order of a few volts. When the sample configuration is dielectrically unstable, as in this study, we have to consider the Fréedericksz torque Γ_F in addition to the GFE torque Γ_G. However, at low voltages only the latter will be significant provided E_a/E_c is large. For instance, for a homogeneous splay distortion and linear scaling of the field, we have

$$\frac{\Gamma_G}{\Gamma_F} = \frac{e^* \sin\theta\cos\theta(\mathrm{d}E/\mathrm{d}z)}{\varepsilon_o\varepsilon_a \sin\theta\cos\theta\, E^2} = \frac{e^*}{\varepsilon_o\varepsilon_a V}\left(\frac{E_a - E_c}{E_a + E_c}\right). \tag{8}$$

With $e^* \sim 10^{-11}\,\mathrm{C\,m^{-1}}$, $\varepsilon_a = 0.1$, $V = 1\,\mathrm{V}$ and $E_a/E_c = 10$, we obtain Γ_G as about nine times Γ_F. Thus we may consider the switching in BEPC at low voltages as primarily a GF response.

Notwithstanding the above interpretation of the low voltage switching, it is possible to view the homogeneous distortion as a special case of the BP instability modified by the GFE. It is shown in [6] that in such a case the BP threshold V_f reduces to V_{fr} and the period of the pattern Λ increases to Λ_m, with

$$V_{fr} = \frac{V_f}{1+\nu}\left(1 - \frac{V_f}{4V_G}\right); \quad \Lambda_m = d\left[\frac{1+\nu}{1-\nu-(V_f/2V_G)}\right]^{\frac{1}{2}}. \tag{9}$$

Evidently, for $2V_G \leqslant V_f/(1-\nu)$, the periodicity of the pattern vanishes. From the earlier mentioned values of k and e at 55°C, and the corresponding values of V_f ($\approx 6.4\,\mathrm{V}$, from figure 3) and ε_a (=0.21 from [12]), we arrive at $\sim 6.4\,\mathrm{V}$ for $V_f/[2(1-\nu)]$; when the GFE threshold is below this limit, the distortion is expected to be homogeneous. The limiting voltage will in general be temperature-dependent since it involves k, e and ε_a.

The GFE considered above assumes a linear field increase between E_c and E_a and it is important to consider whether this condition is fulfilled in practice. For an applied d.c. voltage, the equilibrium field distribution in a weakly conducting nematic is necessarily inhomogeneous, but not linearly varying. Voltage-induced diffuse counterion layers formed next to the electrodes so modify the field that it is homogeneous in bulk and rapidly increasing toward the electrodes in the Debye-like screening layers [20]. Charge injection, which is likely when no blocking layers are applied to the electrodes, will render only the surface field asymmetric, leaving the bulk field uniform [21]. Even when blocking (or aligning) layers are used, the bulk field uniformity is preserved; in this case, selective adsorption of ions of the same sign at these layers could lead to a permanent surface field asymmetry [10]. Differential mobility of the opposite charge carriers also produces a similar field change, except that the surface field asymmetry is now transient [22]. Similar considerations are employed in a recent analysis of the time variation of the field configuration in a nematic cell and its bearing on the transient dielectric response [23].

In applying these ideas to understand the switching in BEPC, we first recognize that a linear field variation across the sample would imply a constant density of injected charges. This condition, generally difficult to fulfill in the presence of ionic impurities in the liquid, is realized to a greater degree in thin samples than in thick ones [21]. In any case, we do observe the GF switching using electrodes coated with blocking layers of polyimide (see later); therefore, besides charge injection, there must be other causes for the bulk field inhomogeneity. As noted earlier, in the equilibrium state, the field gradients due to counterion segregation are likely to be restricted to thin boundary layers; they do not generate observable GF distortions in BEPC and we need examine only the field configurations on the route to equilibrium.

The transient director switch probably involves two counter contributory factors. First, with passage of time, the regions on either side of the midplane $z=0$, wherein the displacement gradient $\mathrm{d}D/\mathrm{d}z$ is non-zero, shrink progressively toward contiguous electrodes. Second, in these regions, $\mathrm{d}D/\mathrm{d}z$ increases simultaneously. Given selective ion adsorption at the electrodes, such as discussed by Thurston [24], these effects are plausible. Consider, for example, positive ions as adsorbed, with a surface charge density, Σ, as in figure 7. In the absence of external bias, diffuse layers

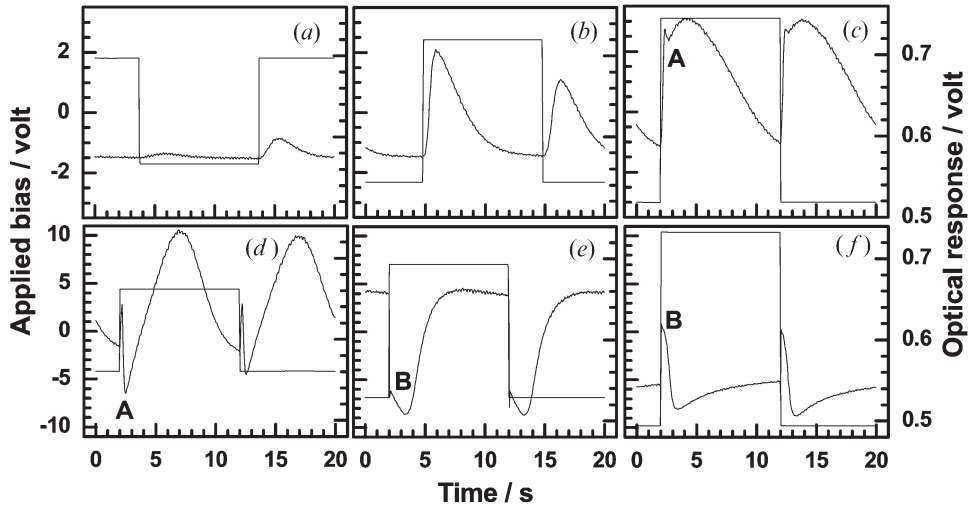

Figure 6. Transient director excursion due to polarity reversal in BEPC driven by a square wave field, at 65°C in a 7.75 μm cell. The voltage-scale (optical response-scale) on the left (right) ordinate is common for (*a*) to (*c*), as also for (*d*) to (*f*). The optical response represents the amplified diode output corresponding to a gain of 10^6.

of negative ions form against these immobile positive ions. The resulting intrinsic double layer field, analysed in detail in [10], would be as shown by the dashed curve. Immediately after applying a d.c. field corresponding to a displacement D_a, the original field is shifted by D_a to the position indicated by the dotted curve. In time, however, the diffuse negative layer next to the cathode is drawn toward the anode, even as the mobile positive ions drift oppositely. Eventually, the equilibrium configuration shown by the continuous curve is obtained. The charging process in itself occupies a very short time, less than a millisecond. But the time for charge drift τ_d across the cell may take a few seconds. For example, from $\tau_d = d^2/(\mu V)$ with μ as the mobility ($\sim 10^{-11}\,m^2\,V^{-1}\,s^{-1}$), for a 8 μm thick sample subject to 1.5 V, τ_d is about 4 s. In this interval, while the transition between the states represented by the dotted and continuous curves takes place, bulk gradients necessary for the transient GF instability are obtained. If injection of charge carriers is also present, the switching effect may be enhanced and long drawn.

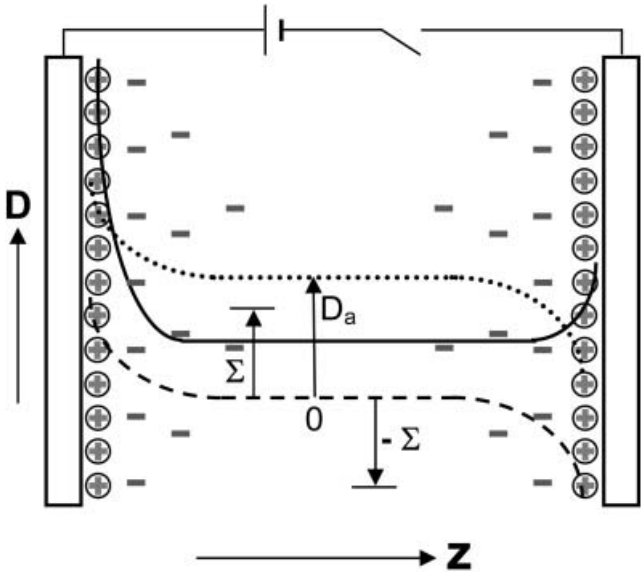

Figure 7. Schematic of the displacement (D) field in the sample at various times approaching equilibrium. Σ denotes the surface charge density of adsorbed ions (⊕) at the electrodes. The D-field is represented by the dashed curve in the absence of bias, dotted curve immediately after applying a bias corresponding to D_a, and continuous curve in the equilibrium state.

The time τ_m of occurrence of the maximum tilt after polarity reversal is found to decrease with increasing bias voltage, as shown in figure 8. It is to be noted that τ_m corresponds to the position of peak intensity only at lower voltages at which only a single maximum occurs in transmission, as in figures 6 (*a*) and 6 (*b*) for example; but for higher voltages when two maxima (minima) are present, τ_m corresponds to the position of the intermediate minimum (maximum), such as position 'A' in figures 6 (*c*) and 6 (*d*), or B in figures 6 (*e*) and 6 (*f*). The inset in figure 8 demonstrates the linearity of $1/\tau_m$ in V, which in turn reflects the involvement of carrier transport velocity in the time-occurrence of maximum δ.

The peak-value of the transmitted intensity profile, for voltages close to the threshold, is linear in applied voltage as seen in figure 9. It is also clear from this figure that after polarity reversal several seconds are

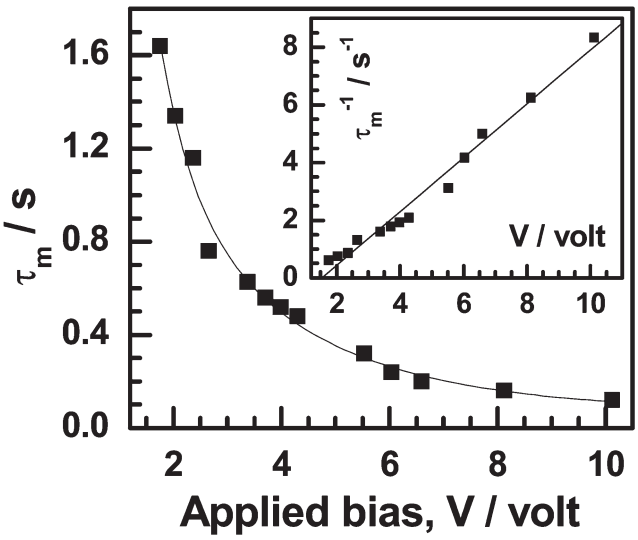

Figure 8. The time of occurrence τ_m of maximum phase change after polarity reversal as a function of voltage. The inset shows a near linear dependence of $1/\tau_m$ on V.

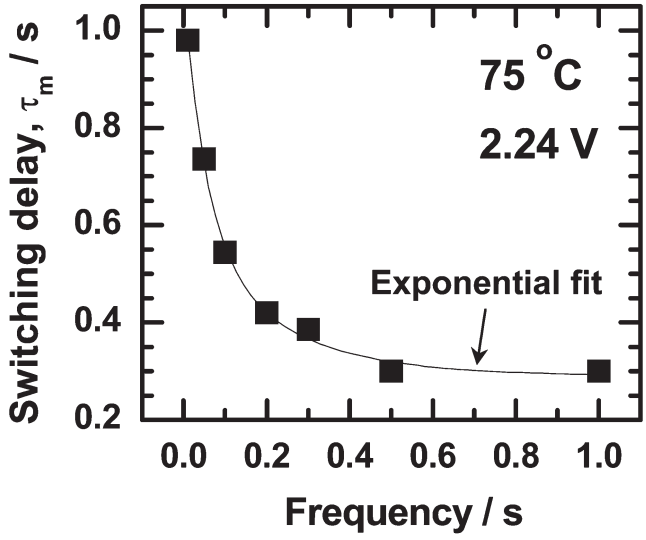

Figure 10. The time of occurrence τ_m of maximum phase change after polarity reversal as a function of frequency.

required for the complete recovery of the steady state. Not surprisingly, therefore, a lowering of the period of the applied waveform will influence the transient behaviour. This is evident from figure 10, showing an exponential decay of the delay time τ_m with increase in frequency. Beyond 1 Hz, the optical response becomes rather irregular.

The switching delay τ_m reduces with increasing temperature as in figure 11, and this is clearly due to the negative temperature coefficient of rotational viscosity. In figure 12, we present the temperature dependence of the gradient flexothreshold V_G and, interestingly, the trend here is quite the reverse compared with V_f in figure 3. Equation (7) requires V_G to exhibit the same temperature behaviour as k/e^* under steady gradient conditions. However, when the gradients are unsteady and the director tilt is

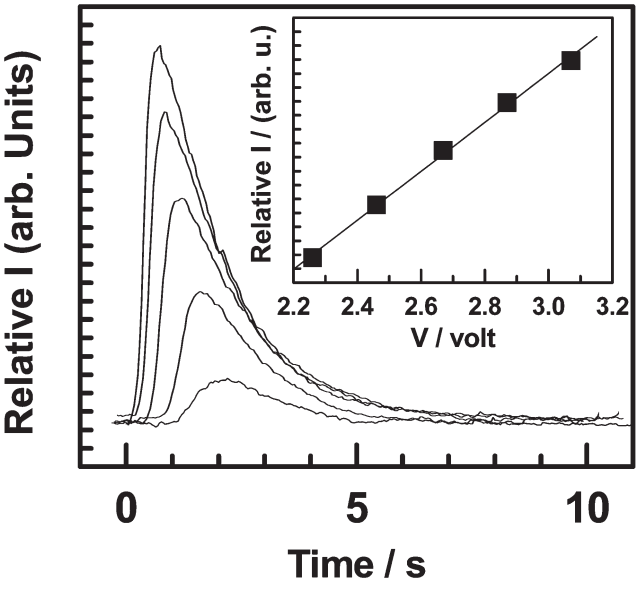

Figure 9. Optical transmission profiles which, in the order of increasing peak height, correspond to 2.26, 2.46, 2.67, 2.87 and 3.07 volts. The inset shows the linear scaling of peak intensity with voltage.

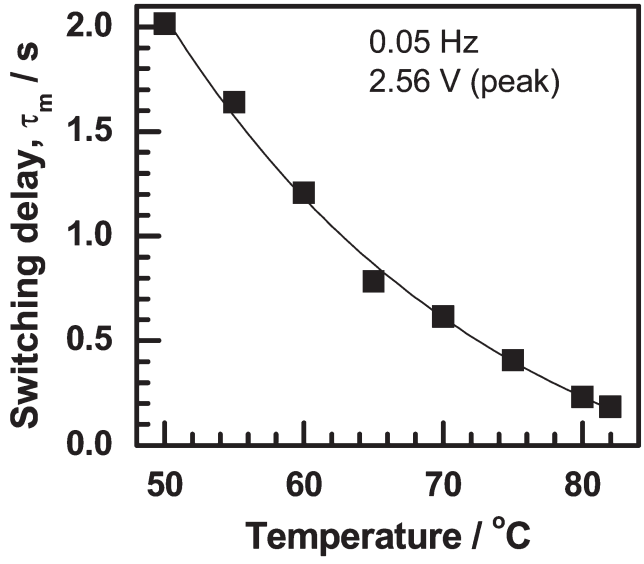

Figure 11. Temperature dependence of switching delay under square wave excitation. The continuous curve is an exponential fit. $d=7.75\,\mu m$.

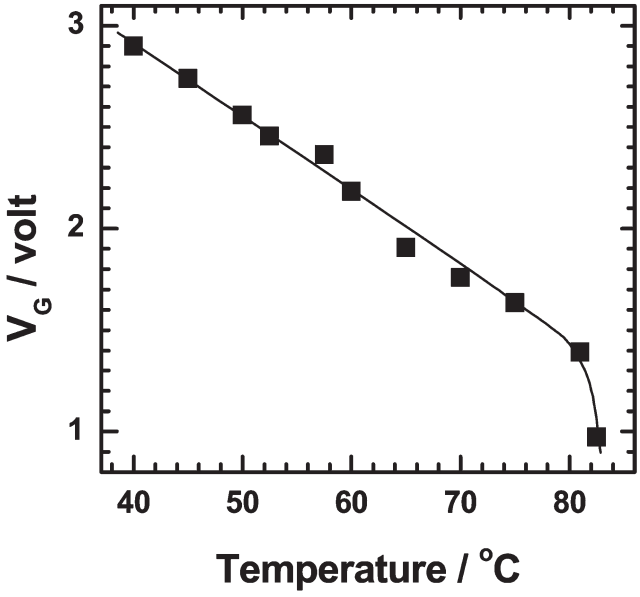

Figure 12. Temperature variation of the threshold of gradient flexoelectric instability. d=7.75 µm.

time-varying, the rotational viscosity will also play a part. In figure 12, the threshold is seen to reduce almost linearly with temperature except close to the nematic–isotropic point where a sudden drop in V_G occurs.

At this point, it is relevant to mention that the threshold V_G is quite sensitive to the boundary conditions. With prolonged use of the sample, over several days, as noted early in [7], the nematic molecules are likely to be adsorbed at the interfaces leading to a lowered anchoring energy or 'softer' boundaries. This would bring down the V_G value. We found in some aged BEPC samples the threshold reducing to as low as 50 mV.

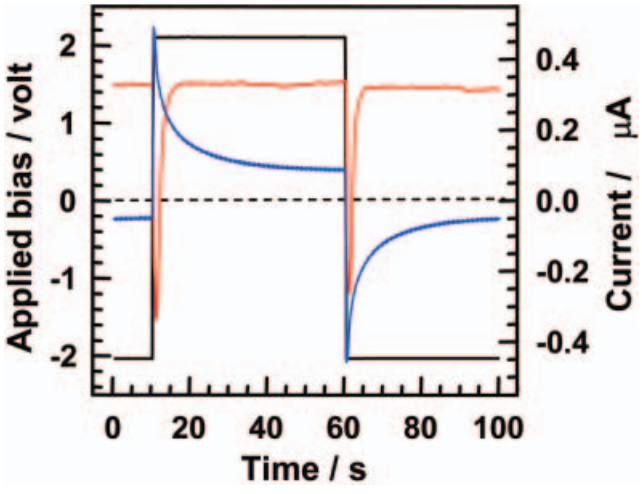

Figure 13. Simultaneous recording of the profiles corresponding to applied bias (in black), current flow through a 100 kΩ series resistor (in blue) and optical transmission (in red) at 75°C. The transmittance is in arbitrary units.

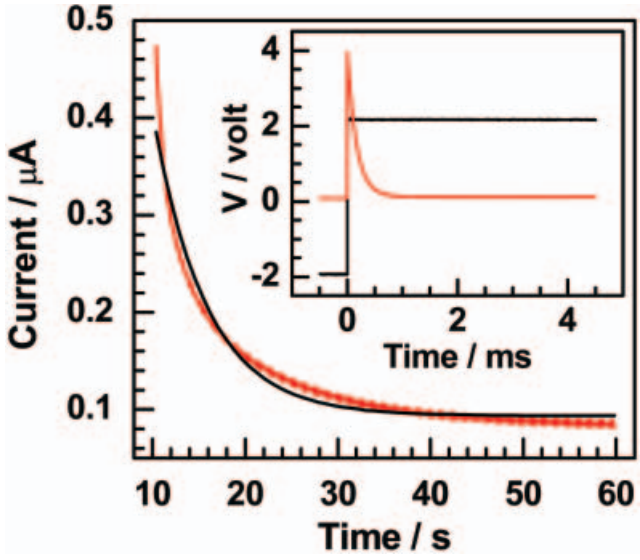

Figure 14. Current through a 100 kΩ series resistor as a function of time during one half cycle of a 10 mHz applied square wave field. The experimental trace is in red; the curve in black represents the exponential fit. In the inset, the red profile shows the voltage across the resistor as a function of time during the initial few seconds after polarity reversal; the corresponding applied voltage step is in black.

In order to examine the nature of current flow subsequent to polarity reversal, we monitored the time variation of voltage across a 100 kΩ series resistor, simultaneously with that of optical transmission. Figure 13 shows a typical set of the profiles recorded. The peak corresponding to capacitor recharging, shown separately in the inset to figure 14, is followed by the ionic current curve. The latter decays approximately in an exponential manner as indicated in figure 14. The residual steady current found in the latter part of each half-cycle is attributable to ions generated through field-induced dissociation of the molecules as well as charge injection. This current increases nonlinearly with V, as in figure 15.

As previously mentioned, transient switching is also observed when the electrodes are coated with aligning polyimide layers. An optical response typical of this case is seen in figure 16. From the viewpoint of charge injection effects, it is noteworthy that the profiles here are narrower and more symmetrical compared with the corresponding ones in figure 6 (*b*) for non-blocking electrodes. Additionally, the switching delay τ_m is now considerably reduced at lower voltages relative to the non-blocking case, although its saturation value at

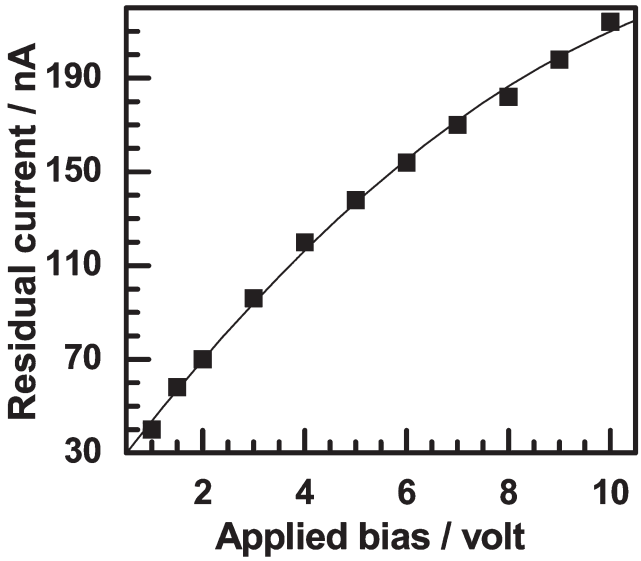

Figure 15. Residual current at the end of switching as a function of voltage. The continuous curve represents the second order polynomial fit. d=7.75 μm.

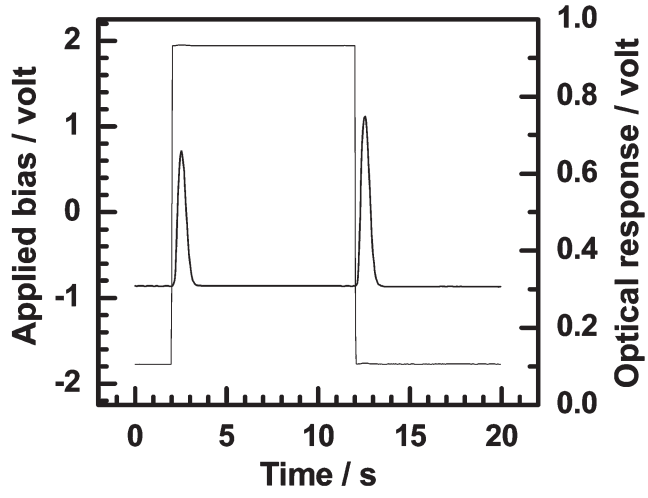

Figure 16. Transient switching response in a 6.7 μm thick layer of BEPC held at 75°C between polyimide-coated electrodes and driven by a 0.05 Hz square wave field. P(45)-A(135). The relative intensity of transmitted light (right hand scale) reveals a momentary birefringence change following each polarity reversal.

higher voltages is not much altered. For instance at 2 V, τ_m is about 1.35 s for the uncoated electrodes (figure 8), but only 0.35 s for the coated electrodes.

The switching properties thus far described may now be compared with those reported in [11] by Basappa and Madhusudana. They employed nematics with rather strong ε_a in the range 8–22, in the dielectrically stable (homeotropic) geometry; BEPC, which is weak in ε_a, is studied here in the dielectrically unstable configuration but well below the experimental Freedericksz threshold (~10 V at 75°C [25]). In [11], the field frequency is high (256 Hz) so that the BP instability is not expected to occur; with BEPC, no GF response was found at all above ~1 Hz and, below this limit, BP modulations occurred at sufficiently high voltages. Very importantly the optical signals in [11] are weak, with the transmittance between crossed polarizers being limited to a few percent; this is attributed to the switching restricted to a thin surface layer corresponding to the electric coherence length of ~0.1 μm. In BEPC, the path change near the threshold is about 100 nm (see figure 5) and the equivalent of the sample thickness is about 1 μm. Such a large path variation indicates a bulk distortion rather than a surface distortion. Further, the switching threshold of 3–6 V μm^{-1} in [11] coincides with the field at which the residual current saturates; such a correlation is absent in BEPC and, as shown in figure 15, the steady current shows no saturation even up to 10 V. Finally, in [11] no switching is observed above 12–15 V μm^{-1}, this field limit being set mainly by the stabilizing Fréedericksz torque overtaking the destabilizing GF torque. In this study there is no such limiting field since the geometry is unstable both dielectrically and flexoelectrically.

4. Concluding remarks

BEPC is capable of displaying inverse flexoelectric, dielectric and electroconvective instabilities under suitable conditions of excitation. The latter two become dominant when the driving field has a frequency exceeding about 25 Hz [25]. Flexoinstability, as demonstrated in this study, becomes important in thin samples (with short director relaxation times), driven by static or very low frequency fields. Under d.c. excitation, BEPC exhibits the Bobylev–Pikin volume instability at a threshold which is temperature-dependent. More interestingly, on subjecting BEPC to low frequency fields of voltage amplitude well below the Fréedericksz threshold, it undergoes a transient GF distortion soon after each polarity reversal. This phenomenon, characterized here mainly in terms of the corresponding electro-optic response, is thought to arise from two factors which contribute oppositely to the director distortion. First, with time, the field gradients that develop in the bulk progressively recede to the boundary regions leaving the field homogeneous in the bulk and this reduces the overall effect. Second, the degree of the gradient in the regions where they exist continues to rise until equilibrium is attained and this contributes positively to the distortion amplitude. These effects are easy to envisage given the existence of intrinsic double layers due to selective ion absorption.

Acknowledgments

We are grateful to Dr S. Krishna Prasad (Centre for Liquid Crystal Research, Bangalore) and Professor N. V. Madhusudana (Raman Research Institute, Bangalore) for their keen interest in this investigation. We are indebted to M/s Eastman Organic Chemicals for supplying, free of charge, the sample of BEPC used in this study.

References

[1] R.B. Meyer. *Phys. Rev. Lett.*, **22**, 918 (1969).
[2] J. Prost, J.P. Marcerou. *J. Phys. Fr.*, **38**, 315 (1977).
[3] A.G. Petrov. In *Physical Properties of Liquid Crystals: Nematics*, D.A. Dunmur, A. Fukuda, G.R. Luckhurst (Eds), Chap. 5.5, INSPEC-IEE, London (2001).
[4] S.A. Pikin. *Structural Transformations in Liquid Crystals*, Chap.V, Gordon and Breach, New York (1991).
[5] A.I. Derzhanski, A.G. Petrov, H.P. Hinov, B.L. Markovski.. *Bulg. J. Phys.*, **1**, 165 (1974).
[6] A. Derzhanski, A.G. Petrov. In *Advances in Liquid Crystal Research and Applications*, Vol. 1, L. Bata (Eds), Pergamon Press, Oxford (1980).
[7] A.I. Derzhanski, A.G. Petrov. *Acta Phys. Pol.*, **A55**, 747 (1979).
[8] H.Y. Chen, K.X. Yang, W. Lee. *Opt. Express*, **12**, 3806 (2004).
[9] H. Naito, K. Yoshida, M. Okuda, A. Sugimura. *J. appl. Phys.*, **73**, 1119 (1993) and references therein.
[10] R.N. Thurston, J. Cheng, R.B. Meyer, G.D. Boyd. *J. appl. Phys.*, **56**, 263 (1984).
[11] G. Basappa, N.V. Madhusudana. *Proc. SPIE*, **4147**, 116 (2000).
[12] W.H. de Jeu, Th.W. Lathouwers. *Mol. Cryst. liq. Cryst.*, **26**, 225, 235 (1974).
[13] D. Balzarini, P. Palffy-Muhoray. In *Liquid Crystals and Ordered Fluids*, Vol. 4, A.C. Griffin, J.F. Johnson (Eds), Plenum Press, New York (1984).
[14] Y.P. Bobylev, V.G. Chigrinov, S.A. Pikin. *J. Phys. (Paris)*, **40**(suppl. 4), C3-331 (1979) ; Y.P. Bobylev, S.A. Pikin. *Sov. Phys. JETP*, **45**, 195 (1977).
[15] L.K. Vistin. *Dokl. Akad. Nauk SSSR*, **194**, 1318 (1970); *Kristallografia*, **15**, 594 (1970).
[16] J.M. Pollak, J.B. Flannery. In *Liquid Crystals and Ordered Fluids*, Vol. 2, J.F. Johnson, R.S. Porter (Eds), Plenum Press, New York (1974).
[17] W. Greubel, U. Wolff. *Appl. Phys. Lett.*, **19**, 213 (1971).
[18] M.I. Barnik, L.M. Blinov, A.N. Trufanov, B.A. Umanski. *J. Phys. (Paris)*, **39**, 417 (1978).
[19] P.R. Maheswara Murthy, V.A. Raghunathan, N.V. Madhusudana. *Liq. Cryst.*, **14**, 483 (1993).
[20] G. Barbero, D. Olivero, N. Scaramuzza, G. Strangi, C. Versace. *Phys. Rev. E*, **69**, 021713 (2004).
[21] Sun Lu, D. Jones. *Appl. Phys. Lett.*, **16**, 484 (1970).
[22] R.N. Thurston, J. Cheng, R.B. Meyer, G.D. Boyd. *J. appl. Phys.*, **56**, 263 (1984).
[23] M. Scalerandi, P. Pagliusi, G. Cipparrone, G. Barbero. *Phys. Rev. E*, **69**, 051708 (2004).
[24] R.N. Thurston. *J. appl. Phys.*, **55**, 4154 (1984).
[25] Pramoda Kumar, K.S. Krishnamurthy. *Phys. Rev. E*, **74**, 031705 (2006).